Journal of Power and Energy Engineering, 2026, 14(11), 123-140
https://www.scirp.org/journal/jpee
ISSN Online: 2327-5901
ISSN Print: 2327-588X

Numerical Simulation of the Performances of a Perovskite-Based Photovoltaic Solar Cell as a Function of Absorber Layer Thickness and Temperature

Daouda Oubda, Pingdewinde Sawadogo, Soumaila Ouedraogo, Hamidou Barry, Boureima Sawadogo

Materials and Environment Laboratory (LAME), Joseph Ki-Zerbo University, Ouagadougou, Burkina Faso
Email: daoudaoubd@gmail.com

How to cite this paper: Oubda, D., Sawadogo, P., Ouedraogo, S., Barry, H. and Sawadogo, B. (2026) Numerical Simulation of the Performances of a Perovskite-Based Photovoltaic Solar Cell as a Function of Absorber Layer Thickness and Temperature. *Journal of Power and Energy Engineering*, **14**, 123-140.
https://doi.org/10.4236/jpee.2026.1411009

Received: October 17, 2026
Accepted: November 17, 2026
Published: November 26, 2026

Copyright © 2026 by author(s) and Scientific Research Publishing Inc.
This work is licensed under the Creative Commons Attribution International License (CC BY 4.0).
http://creativecommons.org/licenses/by/4.0/
Open Access

Abstract

Against an international backdrop characterized by excessive energy consumption, particularly of fossil fuels and by global warming, environmental pollution, and ozone layer depletion, questions remain regarding the development of an abundant, non-polluting energy source that aligns with sustainable development and accelerated growth strategies. This study addresses this context by focusing on optimizing the performance of a perovskite-based photovoltaic (PV) cell, specifically by analyzing the impact of absorber layer thickness and temperature with the aim of developing lightweight, stable, and high-efficiency solar cells. To achieve this, we employed a numerical simulation approach using the one-dimensional solar cell simulation software SCAPS-1D. The study involved analyzing the effects of these physical parameters to identify the critical values that maximize performance. Results obtained using the SnO_2:F/TiO_2/IDL$_1$/$CH_3NH_3PbI_{3x}Cl_x$/IDL$_2$/Spiro-OMeTAD PV structure demonstrated that electrical parameter values rose substantially, with the exception of the fill factor (FF), which peaked at 85.76% at a thickness of W_{abs} = 0.2 µm. The results obtained can be explained by the fact that, as the thickness of the absorber layer increases, a significant number of photogenerated electron-hole pairs are produced from the incident photons absorbed within that layer. Furthermore, this large quantity of electron-hole pairs is efficiently collected at the contacts. For W_{abs} > 0.7 µm, a small fraction of these photogenerated carriers undergoes recombination. The observed decline in open-circuit voltage as temperature increases, which leads to a significant reduction in conversion efficiency, can be explained by a narrowing of the bandgap in the absorber layer, as well as a high recombination rate of photogenerated charge carriers. We adopt

the following values for our solar cell structure model, V_{oc} = 1.10 V, J_{sc} = 22 mA/cm^2, FF = 85.43%, and η = 20.72% for a thickness of 0.4 μm at 300 K, thereby meeting the aim of designing lightweight, stable, high-performance, and low-cost solar cells. In future work, we will investigate the influence of the electron affinity and the bandgap of the absorber layer to further optimize performance.

Keywords

Thin Films, Perovskite, Absorber Layer, Numerical Simulation, SCAPS-1D

1. Introduction

Energy lies at the heart of all human activity; its transformation has been and remains a major concern. Energy, in its various forms, has always been an essential factor in development. It powers households, supports industrial activities, sustains transport systems, and plays a pivotal role in economic and social growth.

Against an international backdrop characterized by excessive energy consumption, particularly of fossil fuels and by global warming, environmental pollution, and ozone layer depletion, questions remain regarding the transition to an abundant, non-polluting energy source that aligns with sustainable development and accelerated growth strategies.

However, faced with steadily rising global energy demand, conventional energy sources, primarily fossil fuels and nuclear power, are revealing their limitations. In 2017, these non-renewable resources still accounted for approximately 86% of global energy consumption and nearly 48% in Africa [1]. Their intensive exploitation entails severe environmental consequences, notably pollution, greenhouse gas emissions, and the gradual depletion of natural reserves [1] [2].

In this context, the use of renewable energy emerges as an essential alternative that is sustainable, clean, and abundant. Among these sources, solar PV energy stands out due to its exceptional potential and the variety of photovoltaic technologies available for its exploitation [2] [3]. In recent decades, significant attention has been focused on perovskite solar cells (PSCs) due to their remarkable properties, such as strong optical absorption, tunable bandgap, ease of synthesis and fabrication, low production costs, and high efficiency. Within a single decade, the PV conversion efficiency of PSCs has risen from approximately 2.2% to over 22% [4] [5].

Despite this promising performance, perovskite solar cells remain sensitive to several physical parameters, particularly the thickness of the absorber layer and the operating temperature [6] [7]. These parameters directly influence the mechanisms of charge carrier generation, transport, and collection, and consequently, the overall performance of the device [8] [9].

It is against this backdrop that the present study is conducted; it focuses on optimizing the performance of perovskite-based solar cells with respect to absorber

layer thickness and temperature, aiming to develop solar cell designs that are lightweight, stable, and highly efficient. To achieve this goal, we adopted a numerical simulation approach using the one-dimensional solar cell simulation software SCAPS-1D. The process involves investigating the effects of these physical parameters to identify the critical values that optimize the performance of thin-film perovskite solar cells. The software enables the modeling of the electrical behavior of multilayer photovoltaic devices by taking into account the optical, electronic, and thermal properties of the materials, thereby offering a reliable approach for predicting performance prior to experimentation [10].

2. Materials and Methods

2.1. Structure of the Perovskite PV Solar Cell

In this article, we consider a perovskite solar cell model with a multilayer structure, illustrated in Figure 1 and described by the following stack: Front contact/SnO_2:F/TiO_2/IDL1/$CH_3NH_3PbI_3Cl_x$/IDL_2/Spiro-OMeTAD/Back contact.

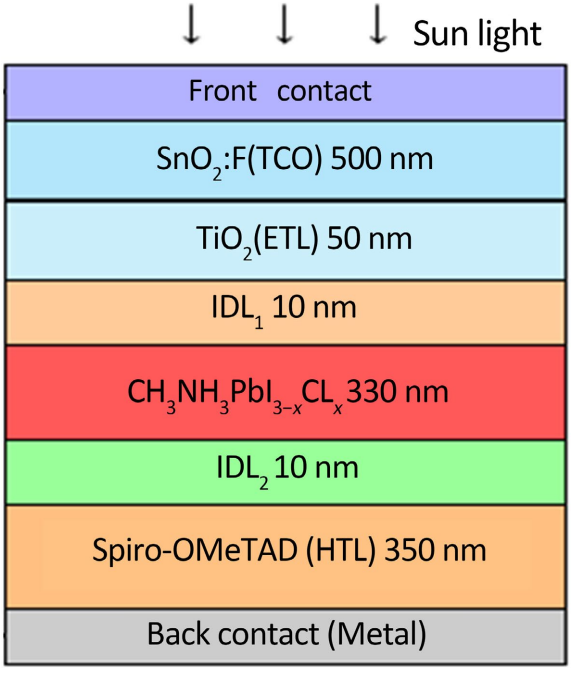

Figure 1. Structure of the perovskite solar cell.

The role of each layer is as follows (Figure 1):

- Front contact: This is the top transparent electrode. Its role is to collect electrons while allowing the maximum amount of sunlight to pass through to the cell absorbing layers.
- SnO_2:F (FTO): Fluorine-doped tin oxide serves as a transparent conductive oxide (TCO) layer due to its high electrical conductivity and optical transparency. Its primary role is to ensure electrical conduction to the front contact while maintaining maximum optical transparency to maximize photon

intake.

- TiO_2: Titanium dioxide acts as an electron transport layer (ETL). It selectively extracts electrons generated by the perovskite and transports them to the front electrode, while effectively blocking the passage of holes to prevent recombination. Titanium dioxide (TiO_2) functions as a buffer layer [5] [11].
- IDL_1 (Interfacial Layer 1): This interfacial layer serves to passivate surface defects between the TiO_2 and the perovskite. Its role is to improve energy band alignment, reduce charge recombination losses at this critical junction, and optimize electron transfer. This layer enables realistic modeling of charge carrier recombination phenomena at the TiO_2 interface and plays a decisive role in the device's overall performance [11] [12].
- $CH_3NH_3PbI_{3x}Cl_x$: This layer, composed of a mixed organic-inorganic halide perovskite, is the cell's primary absorbing material. Its role is to capture sunlight photons to generate electron-hole pairs (excitons), which are subsequently separated to produce electric current. This layer is known for its high absorption coefficient and its ability to efficiently generate charge carriers [13].
- IDL_2 (Interfacial Layer 2): Located between the perovskite and Spiro-OMeTAD, this second interfacial layer reduces surface defects at this boundary. It prevents chemical degradation of the absorber material, minimizes charge recombination, and facilitates hole extraction. This layer enables realistic modeling of charge-carrier recombination phenomena at the interface with Spiro-OMeTAD and plays a crucial role in the device's overall performance [11] [12].
- Spiro-OMeTAD: This organic material serves as the hole transport layer (HTL); it is widely used due to its favorable electronic properties and good compatibility with perovskite materials. Its role is to selectively extract holes from the perovskite and transport them to the back contact, while acting as an insulating barrier to block the flow of electrons [13] [14].
- Back contact: This is the bottom metal electrode, made of gold or silver. Its role is to collect holes to complete the electrical circuit, while reflecting unabsorbed light back into the cell for a second chance at absorption.

2.2. Operating Principle

When sunlight strikes the surface of the solar cell (**Figure 1**), incident photons first pass through the front transparent layers, depending on their energy and the bandgap of each material. High-energy photons (above 3.2 eV) are partially absorbed by the TiO_2 or FTO, whereas photons with energy below 2.5 eV pass easily through these oxide layers without being absorbed [15] [16]. When photons with energies of 2.3 eV or 1.7 eV reach the perovskite absorber layer ($CH_3NH_3PbI_{3-x}Cl_x$), which has a bandgap of approximately 1.55 eV, they are absorbed and converted into charge carriers [17] [18]. Conversely, very low-energy photons (infrared, below 1.5 eV) pass through the absorber without interacting, as their energy is lower than its bandgap. Driven by the internal electric field, the generated electrons migrate through IDL_1 and TiO_2 to be collected by the FTO and the front contact, while

holes move in the opposite direction through IDL_2 and Spiro-OMeTAD toward the back contact, thereby generating a direct electric current [19] [20]. Unabsorbed photons with energies below 1.5 eV are reflected at the back contact back into the cell [21] [22].

2.3. SCAPS-1D Simulation Software

Computer-aided design tools currently play a key role in the study and optimization of complex structures, particularly in the field of PV solar cells. High-performance simulators make it possible to rapidly explore the effects of varying specific physical material parameters, identify the most efficient combinations, and propose concrete improvements to enhance device performance. This not only provides a better understanding of the internal operation of solar cells but also offers manufacturers valuable avenues for optimization [5]. Several one-dimensional simulation software packages have been developed for this purpose, such as SCAPS-1D, AMPS-1D, ASA, PC-1D, and AFORS-HET [10]. They are widely used to simulate thin-film solar cells, such as those based on CdTe, CIGS, GaAs, or a-Si:H. In this study, we used SCAPS-1D software (version 3.3.10), developed at Ghent University, to investigate the impact of absorber thickness and temperature on the performance of perovskite solar cells. SCAPS software calculates the solution to the fundamental semiconductor equations in one dimension under steady-state conditions [10]. These equations include Poisson's equation for the electrostatic potential φ, as well as the electron and hole continuity equations, using approximate boundary conditions [5] [10]. The Poisson equation used for semiconductors is given by:

$$\nabla.\left(\varepsilon\nabla\varphi\right) = -q\left(p - n + N_D^+ - N_A^-\right) \tag{1}$$

The electron and hole continuity equations are, respectively:

$$\nabla.\overrightarrow{j_n} = q\left(R - G\right) + q\frac{\partial n}{\partial t} \tag{2}$$

$$\nabla.\overrightarrow{j_p} = q\left(R - G\right) + q\frac{\partial p}{\partial t} \tag{3}$$

where: ε is the dielectric constant, φ is the electrostatic potential, n and p are the free carrier concentrations (electrons and holes), N_D^+ and N_A^- are the densities of ionized donors and acceptors, $\vec{j}_n$ and $\vec{j}_p$ are the electron and hole current densities, R and G are the charge carrier recombination rate and generation rate, respectively.

Table 1 presents the physical parameters of the various layers.

Table 1. Basic optical and electrical properties of the materials used in the proposed structure perovskite cell properties.

Contacts properties		
	Right	Left
Φ_b [eV]	$\Phi_{bn} = 0.35$	$\Phi_{bp} = -0.0572$

Continued

S_e [cm/s]			10^7		10^7	
S_h [cm/s]			10^5		10^5	
Reflectivity			0.05		0.6	
Layers properties						
Parameters	SnO_2:F	TiO_2	IDL_1	$CH_3NH_3PbI_{3x}Cl_x$	IDL_2	Spiro-OMeTAD
W (nm)	500	50	10	330	10	350
Eg (eV)	3.50	3.20	1.55	1.55	1.55	3.0
χ (eV)	4.0	3.90	3.90	3.90	3.90	2.45
$\varepsilon/\varepsilon_0$	9.0	9.0	6.5	6.5	6.5	3.0
μ_e (cm^2/Vs)	20	20	2	2	2	2×10^{-4}
μ_h (cm^2/Vs)	10	10	2	2	2	2×10^{-4}
N_A [cm^{-3}]	-	-	-	-	-	2×10^{18}
N_D [cm^{-3}]	2×10^{19}	10^{16}	10^{13}	10^{13}	10^{13}	-
N_t	10^{15}	10^{12}	2×10^{17}	2.5×10^{13}	10^{17}	10^{15}
Bulk defects properties						
Parameters		FTO (SnO_2:F)	TiO_2	$CH_3NH_3PbI_{3-x}Cl_x$		Spiro-OMeTAD
σ_e [cm^2]		2×10^{-14}	1×10^{-15}	1×10^{-13}		1×10^{-15}
σ_h [cm^2]		2×10^{-14}	1×10^{-15}	1×10^{-13}		1×10^{-15}
E_A, E_D [eV]		0.60	0.60	0.60		0.10
W_G [eV]		0.10	0.10	0.10		0.10

Note: Φ_b —barrier height ($\Phi_{bn} = E_C - E_F$, $\Phi_{bp} = E_F - E_V$); S —surface recombination velocity; W —layer width; ε —dielectric constant; μ —mobility; E_g —band gap energy; E_A, E_D —peak energy in; σ_e , σ_h —capture cross section electrons and holes; χ_e —electron affinity; W_G —characteristic energy; N_A , N_D —shallow uniform acceptor and donor density; N_t—total defect density [11] [13] [14].

3. Results and Discussion

3.1. Influence of Absorber ($CH_3NH_3PbI_{3x}Cl_x$) Thickness on J-V Characteristics

The solar cell is simulated under standard AM1.5G illumination at a temperature of 300 K, with the absorber layer bandgap set to 1.55 eV, a typical value for lead-iodide-based perovskites, ensuring efficient absorption of the visible solar spectrum.

Figure 2 illustrates the influence of the $CH_3NH_3PbI_{3x}Cl_x$ layer thickness on the solar cell current-voltage (J-V) characteristic.

Numerical simulation results for our PV structure (Front Contact/SnO_2:F/TiO_2/IDL_1/$CH_3NH_3PbI_3Cl_x$/IDL_2/Spiro-OMeTAD/Back Contact) show that as the perovskite absorber thickness increases, the maximum power region of the J-V characteristic expands. This increase becomes progressively less significant at greater absorber layer thicknesses.

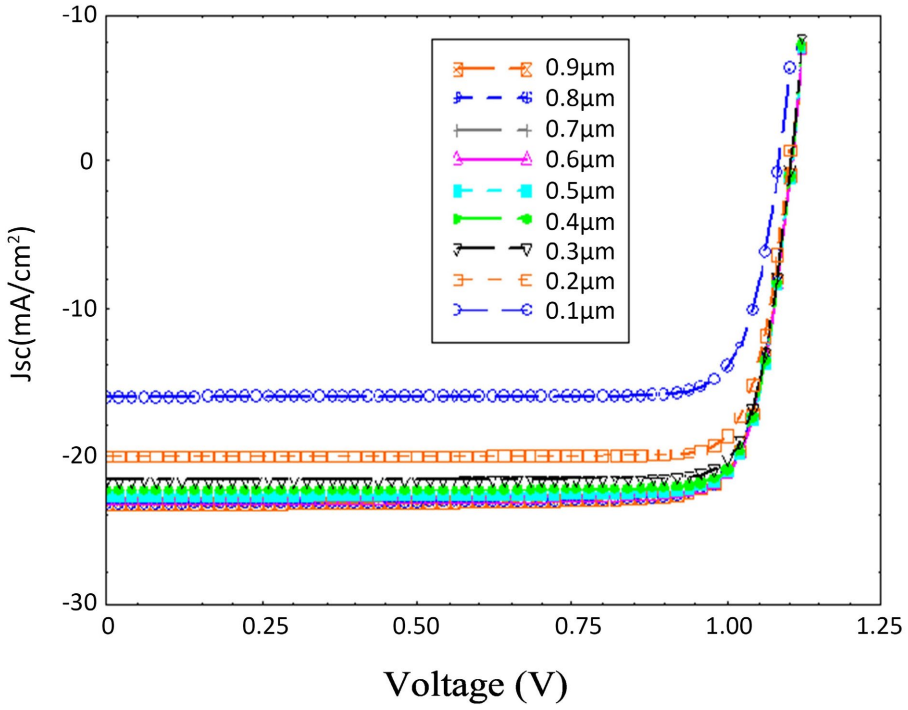

Figure 2. J-V characteristic as a function of $CH_3NH_3PbI_{3x}Cl_x$ absorber thickness.

The increase in the maximum power region graphically corresponding to the area under the curve in the generation quadrant leads to an increase in both the voltage and the current density of the PV solar cell (**Figure 2**). The rise in current density can be attributed to the fact that a thicker perovskite absorber offers a larger volume for interaction with incident light. Consequently, it absorbs a greater fraction of the photon flux, particularly at longer wavelengths. This enhanced absorption generates a larger number of electron-hole pairs. This shifts the entire J-V curve downward, reflecting an overall increase in the extracted electric current density for a given voltage.

As the thickness of the absorber increases, the distance between the space-charge region and the charge-carrier collection contacts (TiO_2 and Spiro-OMeTAD) grows; consequently, for many charge carriers, the diffusion length becomes shorter than this distance. As a result, these charge carriers recombine, while the voltage remains stable or decreases only very slightly due to the increase in bulk recombination. The cell maintains a high voltage level while providing a significantly higher current density.

To better understand the effects of absorber thickness on the performance of our PV structure, we examined the electrical parameters. A quantitative analysis of the electrical parameter curves V_{oc} (**Figure 3**), J_{sc} (**Figure 4**), FF (**Figure 5**), and η (**Figure 6**), derived from the curves in **Figure 2**, shows that V_{oc}, J_{sc}, and the conversion efficiency increase with absorber thickness, approaching a horizontal asymptote for $W_{abs} > 0.7$ µm. In contrast, the FF values reach an optimum of 85.76% at $W_{abs} = 0.2$ µm.

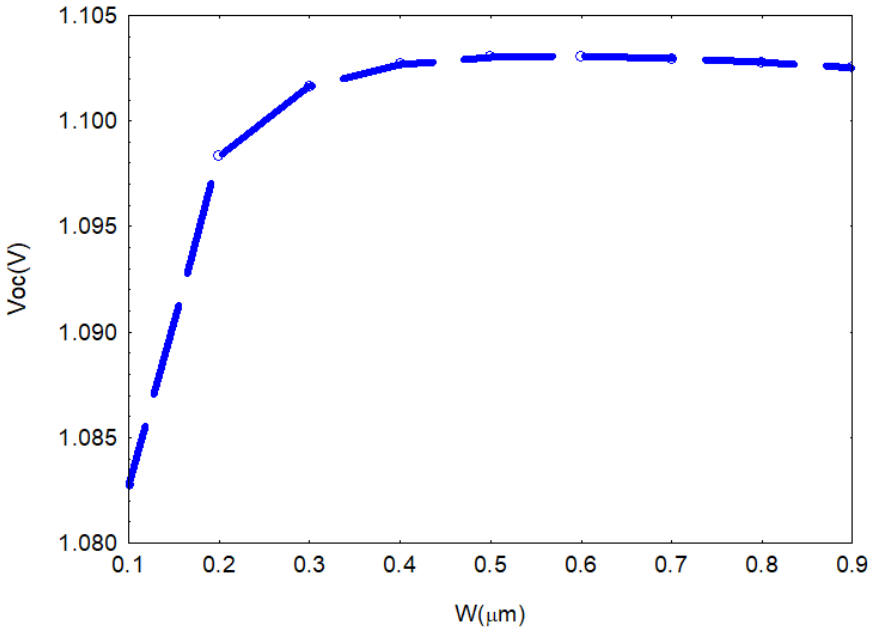

Figure 3. V_{oc} as a function of absorber thickness.

Increasing the absorber volume results in a higher overall density of photogenerated carriers; this raises the electron quasi-Fermi level and lowers the hole quasi-Fermi level, thereby increasing the available voltage.

Additionally, the presence of the IDL_1 and IDL_2 intermediate layers likely plays a key role in suppressing surface/interface recombination, allowing the V_{oc} to increase (**Figure 3**) without being limited by contact losses.

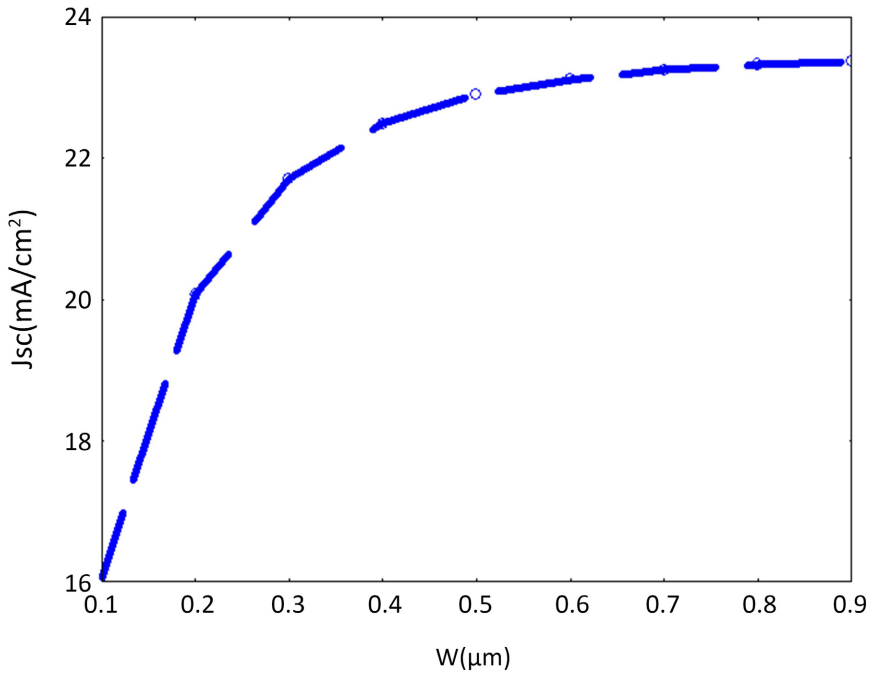

Figure 4. J_{sc} as a function of absorber thickness.

Regarding J_{sc}, increasing the thickness of the perovskite layer results in greater absorption of incident photons, leading to improved generation of electron-hole pairs, particularly at longer wavelengths of the solar spectrum, where the absorption coefficient is very low.

In practical conditions, for J_{sc} to effectively increase with thickness (Figure 4), the diffusion length of charge carriers within the chlorine-doped perovskite ($CH_3NH_3PbI_{3x}Cl_x$) must be equal to or greater than the thickness of the layer. This ensures that charge carriers generated deep within the material can reach the transport layers (TiO_2 and Spiro-OMeTAD) without undergoing recombination.

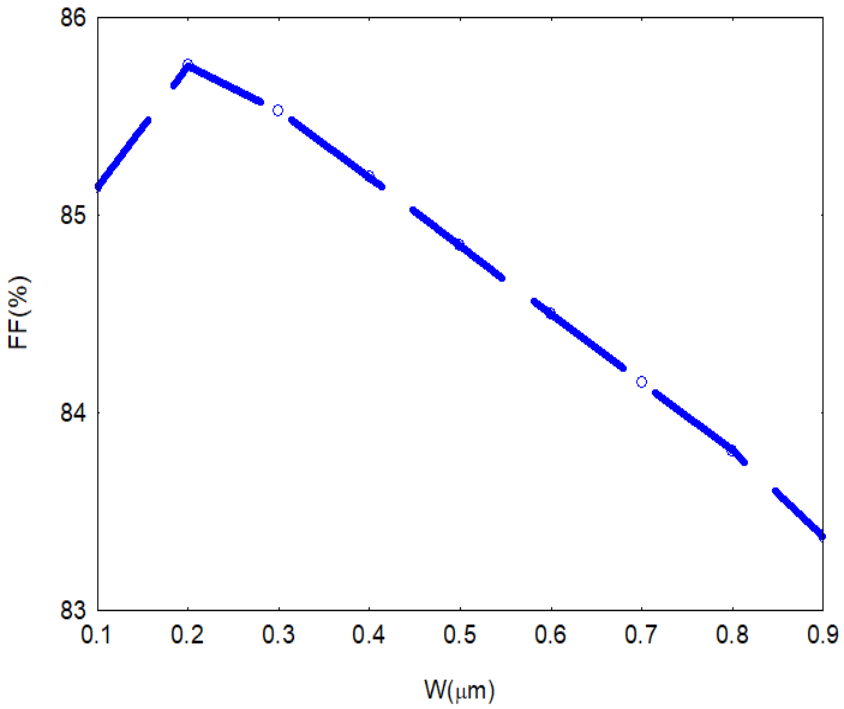

Figure 5. FF as a function of absorber thickness.

The behavior of the fill factor (FF) (Figure 5) reflects a competition between two opposing physical phenomena as the thickness increases:

Before the optimum point in the rising phase, a layer that is too thin leads to leakage currents (shunts). As the layer thickens, film quality improves, shunt resistance (R_{sh}) increases, and interface recombination decreases, causing the FF to rise (Figure 5).

After the optimum point in the declining phase beyond a certain thickness, the device series resistance (R_s) increases because charge carriers must travel a greater distance to be collected. Even with an excellent diffusion length, the increase in internal ohmic resistance eventually degrades the slope of the J-V curve near the maximum voltage, resulting in a decrease in the FF. The value of 85.76% represents the perfect balance between low recombination and low series resistance (Figure 5).

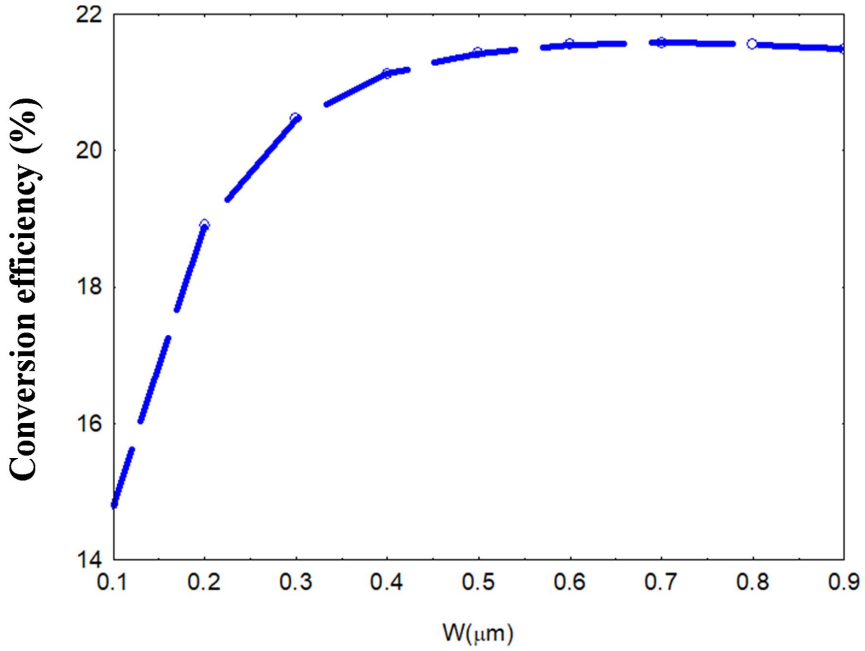

Figure 6. η as a function of the absorber thickness.

Since the overall efficiency of our structure is defined as the ratio of the product of the three electrical parameters to the incident power (**Figure 6**), its significant increase with thickness demonstrates that the gains in optical absorption far outweigh the electrical losses, namely those arising from series resistance, shunt resistance, and charge-carrier recombination.

The results obtained are in good agreement with those reported by Minemoto *et al.* in 2014 [13], highlighting an optimal trade-off between optical absorption and charge-carrier transport when selecting the thickness of the absorbing layer. Consequently, employing a $CH_3NH_3PbI_{3x}Cl_x$ absorber layer of moderate thickness proves to be an effective strategy for strengthening the internal electric field, limiting recombination losses, and facilitating charge-carrier extraction, ultimately leading to an overall improvement in device performance [14] [23].

3.2. Influence of $CH_3NH_3PbI_{3x}Cl_x$ Absorber Thickness on Quantum Efficiency

Figure 7 shows the variation of the external quantum efficiency (EQE) of a perovskite-based photovoltaic solar cell as a function of incident photon wavelength (λ) for various thicknesses (W) of the $CH_3NH_3PbI_{3x}Cl_x$ absorber layer.

In the short-wavelength region (300 nm < λ < 350 nm), a low EQE value is observed. This reduction is primarily attributed to parasitic photon absorption by the SnO_2 transparent conducting oxide (TCO) layer located at the front of the device, which limits the amount of light reaching the active absorber layer [13] [14].

Furthermore, it is observed that the quantum efficiency improves significantly

as the absorber layer thickness increases. This improvement is linked to enhanced optical absorption, allowing a greater number of incident photons to be converted into electron-hole pairs. Consequently, the collection probability of photogenerated charge carriers increases, while bulk recombination losses are reduced [2] [24]. This explains the substantial increase in current density values for our structure and in J_{sc}, as noted in Section 3.1.

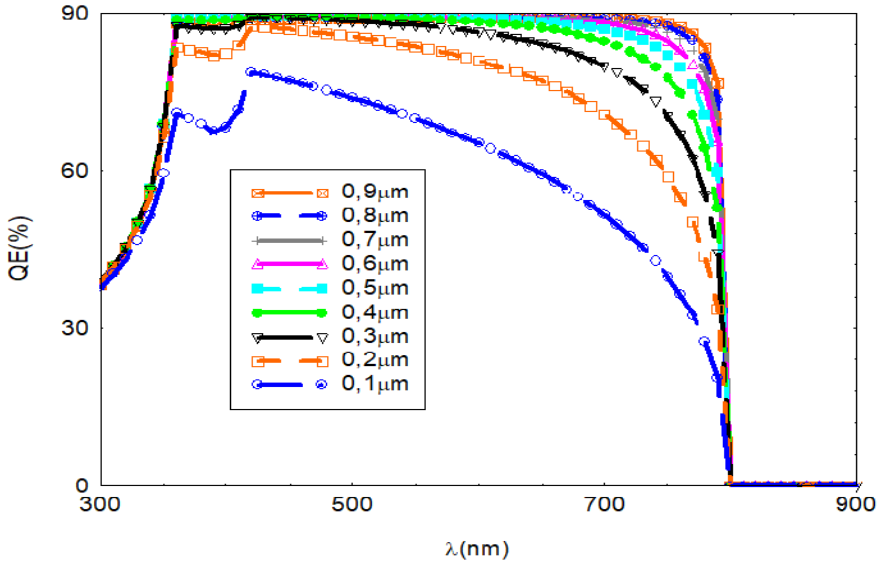

Figure 7. Quantum efficiency as a function of absorber thickness.

A maximum quantum efficiency of approximately 89.40% is achieved at an optimal absorber thickness of W_{abs} = 0.4 µm. Beyond this thickness, the improvement in EQE tends to plateau, reflecting a balance between increased light absorption and limitations related to charge carrier transport and recombination within the perovskite bulk [25] [26].

3.3. Influence of Temperature on the Current Density-Voltage Characteristic and Electrical Parameters

In this section, the solar cell is simulated under standard AM 1.5 G illumination, with an absorber layer thickness of 0.1 µm and a bandgap set to 1.55 eV, a typical value for lead-iodide-based perovskites, ensuring efficient absorption of the visible solar spectrum.

Figure 8 and **Figure 9** show respectively the current density-voltage (J-V) characteristic curves and quantum efficiency of a perovskite-based solar cell at various operating temperatures. These results indicate that the quantum efficiency is virtually independent of temperature (**Figure 9**), suggesting that optical absorption and charge carrier generation processes are not significantly affected by thermal variations within the studied temperature range [1].

Detailed analysis shows that the voltage and current density of our solar PV structure are sensitive to temperature variations (**Figure 8**), as are the electrical param-

eters. In addition, Figure 10 and Figure 11 show that the fill factor and the short-circuit current density also present an important dependence on temperature, at high temperature, parameters such as the electron and hole mobility, carrier concentrations and band gaps of the materials would be affected, which leads to a lower conversion efficiency (Figure 12) [27]. Similarly, the open-circuit voltage (Figure 13) and conversion efficiency (Figure 12) decrease significantly as the temperature increases [2] [6].

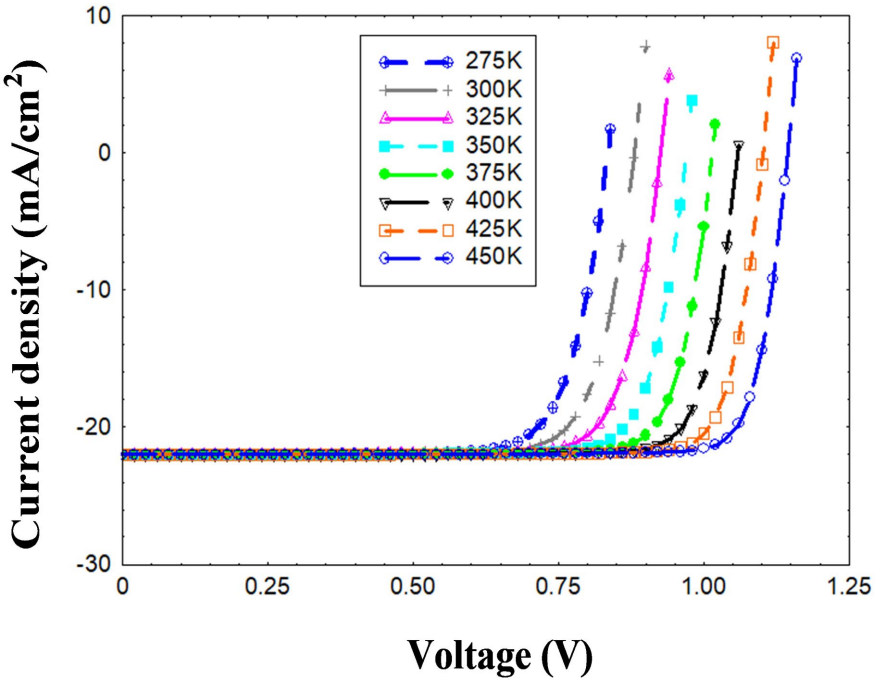

Figure 8. J-V characteristic as a function of temperature.

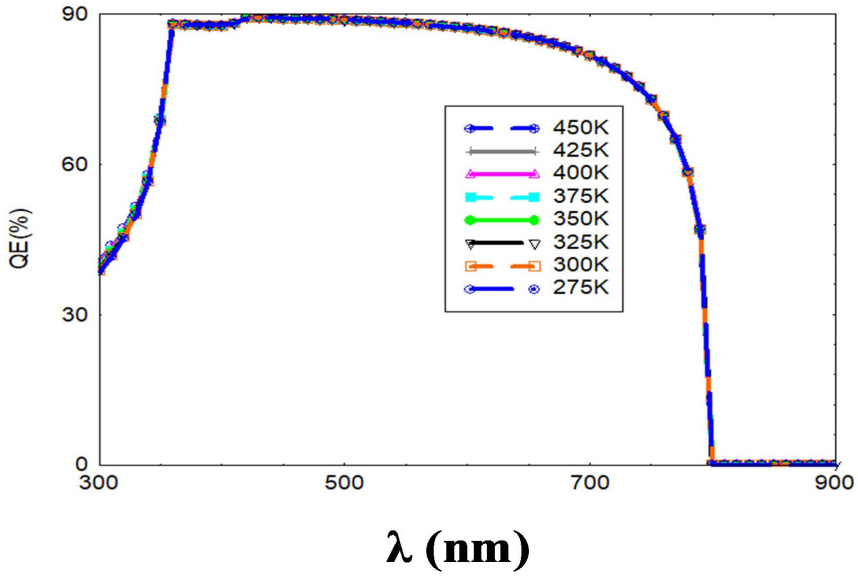

Figure 9. Quantum efficiency as a function of temperature.

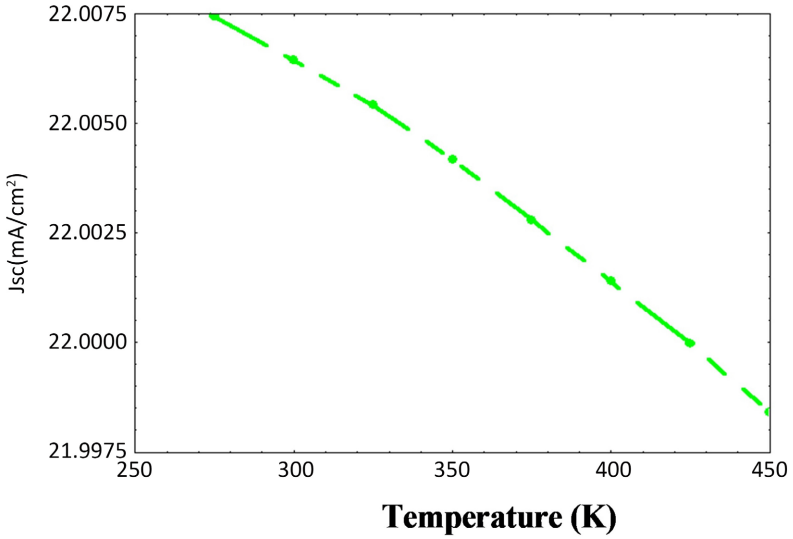

Figure 10. J_{sc} as a function of temperature.

This behavior of the V_{oc} (**Figure 13**) can be interpreted using Equation (4), derived from the diode model applied to the solar cell equivalent electrical circuit. This relationship expresses the open-circuit voltage as a function of temperature:

$$V_{oc} = \frac{E_a}{q} - \left(\frac{AkT}{q}\right)\ln\left(\frac{J_{oo}}{J_{sc}}\right) \tag{4}$$

where E_a denotes the activation energy, q is the elementary charge, A is the diode ideality factor, k is the Boltzmann constant, and J_{oo} is the pre-factor associated with the saturation current density. An increase in temperature raises the logarithmic term of the equation, leading to a decrease in open-circuit voltage and, consequently, in the device overall efficiency.

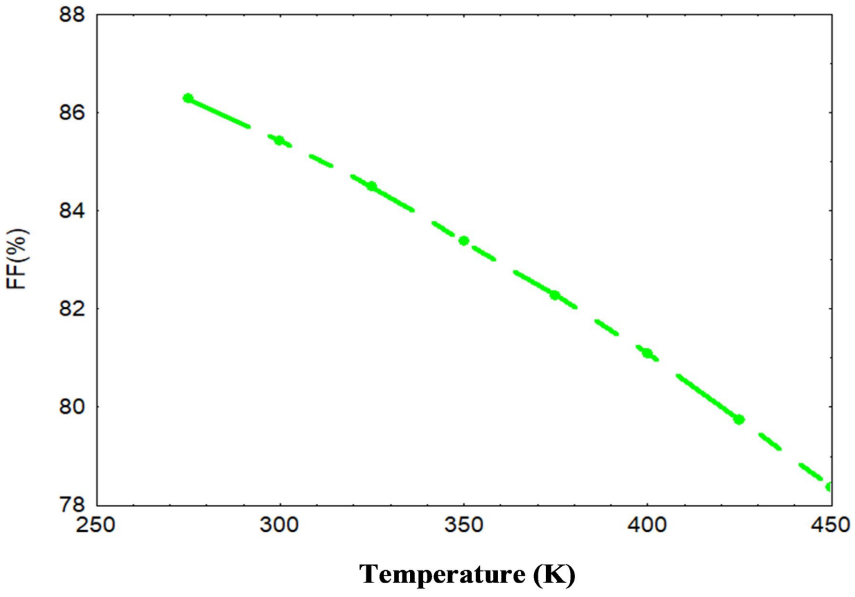

Figure 11. FF as a function of temperature.

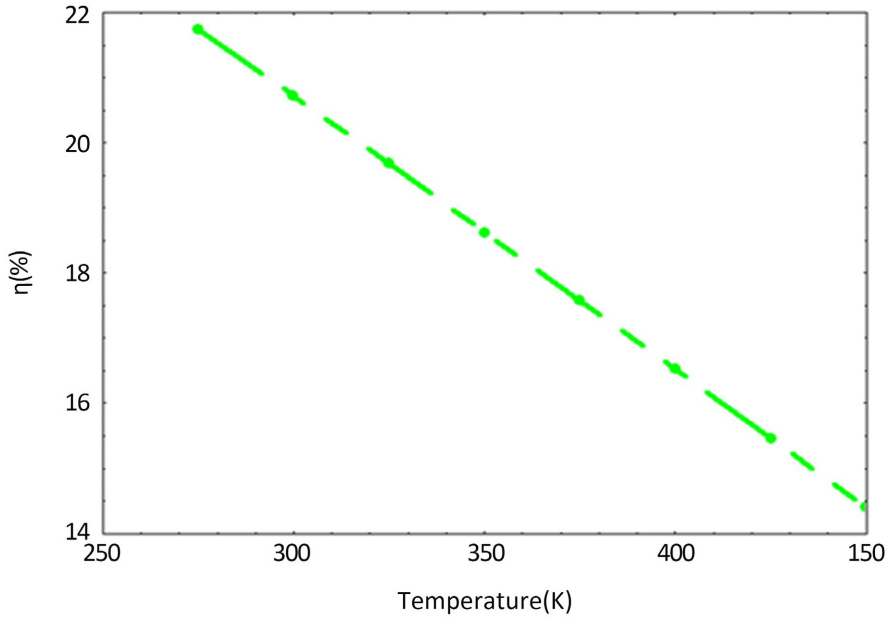

Figure 12. PV conversion efficiency as a function of temperature.

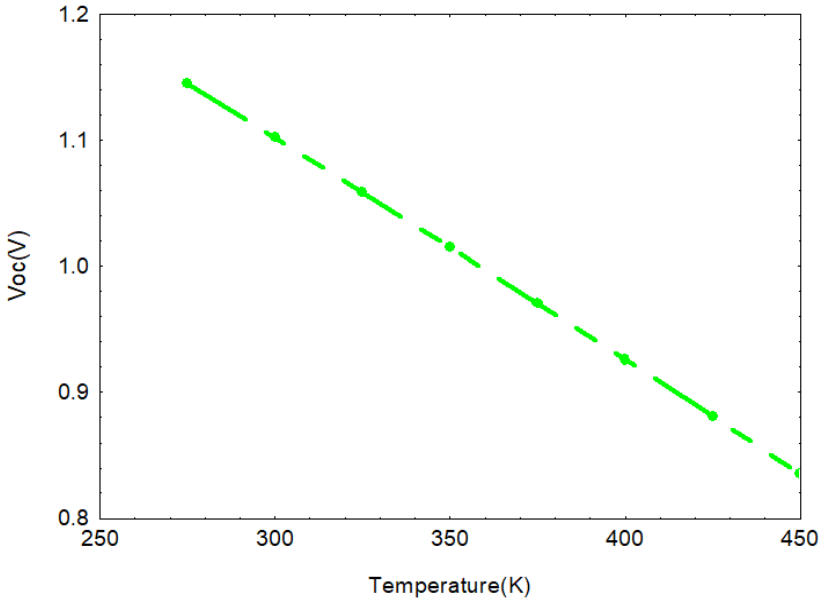

Figure 13. V_{oc} as a function of temperature.

Using the numerical model thus allows for the estimation of key phenomenological parameters such as E_a, A, and J_{oo}, assuming that the short-circuit current density remains practically constant over the temperature range considered. This approach provides a deeper understanding of the thermal impact on the performance of perovskite solar cells [2].

4. Conclusions

In this article, we presented the results of the numerical simulation of a perovskite-

based PV solar cell with the structure SnO_2:F/TiO_2/IDL_1/$CH_3NH_3PbI_{3x}Cl_x$/IDL_2/Spiro-OMeTAD, using SCAPS-1D software. We investigated the influence of the absorber layer ($CH_3NH_3PbI_{3x}Cl_x$) thickness and temperature on the J-V characteristics, electrical parameters (V_{oc}, J_{sc}, FF, and η), and quantum efficiency (QE) of the PV solar cell.

The increase in current density and voltage in the studied solar structure can be explained, on the one hand, by the fact that a thicker perovskite absorber absorbs a larger fraction of the photon flux, particularly at longer wavelengths and generates a greater number of electron-hole pairs. On the other hand, as the absorber thickness increases, the distance between the space-charge region and the charge-carrier collection contacts grows, leading to the recombination of a significant number of charge carriers; the voltage remains stable or decreases only slightly due to increased bulk recombination.

The increase in V_{oc} values can be explained by the rise in the electron quasi-Fermi level and the lowering of the hole quasi-Fermi level. The significant increase in conversion efficiency with thickness demonstrates that the gain in optical absorption far outweighs electrical losses caused by series resistance, shunt resistance, and charge-carrier recombination.

Furthermore, the results show that a well-optimized, ultra-thin absorber ($W_{abs} \leq$ 1000 nm) ensures efficient photon absorption while enhancing the internal electric field. This configuration facilitates the separation and extraction of photogenerated charges while limiting bulk recombination mechanisms. These combined effects result in a significant improvement in short-circuit current density (J_{sc}), open-circuit voltage (V_{oc}), and conversion efficiency (η). Conversely, an increase in operating temperature leads to a notable degradation in the performance of the PV solar cell, specifically a reduction in V_{oc} and conversion efficiency, highlighting the high sensitivity of perovskite solar cells to thermal conditions.

This study also highlights that the combination of an ultra-thin absorber layer and appropriate thermal management serves as an effective strategy for enhancing both the performance and stability of perovskite solar cells under real-world operating conditions, thereby addressing the goal of designing lightweight, high-performance, stable, and low-cost solar cells. In this context, we adopt the following values for our solar cell structure model: V_{oc} = 1.10 V, J_{sc} = 22 mA/cm^2, FF = 85.43%, and η = 20.72% at 300 K, with an absorber thickness of 0.4 μm (falling within the range 0.3 μm ≤ W_{abs} ≤ 0.6 μm). In future research, we will investigate the effects of electron affinity and the absorber bandgap to optimize performance.

Author Contributions

Daouda Oubda: Conceptualization, Data curation, Formal analysis, Funding acquisition, Investigation, Methodology, Resources, Software, Supervision, Validation, Visualization, Writing—original draft, Writing—review & editing.

Pingdewinde Sawadogo: Conceptualization, Formal analysis, Data curation, Methodology, Project administration, Resources, Supervision, Validation, Writ-

ing—original draft, Writing—review & editing.

Soumaila Ouedraogo: Conceptualization, Data curation, Formal analysis, Funding acquisition, Investigation, Methodology, Project administration, Resources, Software, Validation.

Hamidou Barry: Conceptualization, Data curation, Formal analysis, Funding acquisition, Investigation, Methodology, Software, Supervision, Validation, Project administration, Resources.

Boureima Sawadogo: Conceptualization, Data curation, Formal analysis, Funding acquisition, Methodology, Project administration, Resources, Supervision, Validation, Visualization.

Conflicts of Interest

The authors declare no conflicts of interest regarding the publication of this paper.

References

[1] Oubda, D., Ouédraogo, S., Diasso, A., Kébré, M.B., Zougmoré, F., Koalga, Z., *et al.* (2022) Renewable Energies in Africa, Context and Socio-Economic Challenge. *Open Journal of Applied Sciences*, **12**, 1856-1872. https://doi.org/10.4236/ojapps.2022.1211128

[2] Kebre, M.B., Zougmore, F., Oubda, D., Ouedraogo, S. and Koalaga, Z. (2012) Energy and Development in the South. *Paper No.* 6, *International Francophone Symposium on Energetics and Mechanics* (*CIFEM*), Ouagadougou, 2-4 May 2012, 103-108.

[3] Lincot, D., Collin, S., Even, J. and Kleider, J. (2015) Silicium, Couches Minces, Pérovskites, Photonique: De Nouvelles Avancées de la Recherche sur les Cellules Photovoltaïques. Un Bon Signe pour la COP 21. *Photoniques*, **78**, 23-27. https://doi.org/10.1051/photon/20157823

[4] Tong, X., Lin, F., Wu, J. and Wang, Z.M. (2016) High Performance Perovskite Solar Cells. *Advanced Science*, **3**, Article ID: 1500201.

[5] Yue, L., Yan, B., Attridge, M. and Wang, Z. (2016) Light Absorption in Perovskite Solar Cell: Fundamentals and Plasmonic Enhancement of Infrared Band Absorption. *Solar Energy*, **124**, 143-152. https://doi.org/10.1016/j.solener.2015.11.028

[6] Bush, M.E., Sims, J.D., Erickson, S.S., VanSant, K.T., Ghosh, S., Luther, J.M., *et al.* (2025) Space Environment Considerations for Perovskite Solar Cell Operations: A Review. *Acta Astronautica*, **235**, 235-250. https://doi.org/10.1016/j.actaastro.2025.05.025

[7] Ouslimane, T., Et-taya, L., Elmaimouni, L. and Benami, A. (2021) Impact of Absorber Layer Thickness, Defect Density, and Operating Temperature on the Performance of MAPbI3 Solar Cells Based on ZnO Electron Transporting Material. *Heliyon*, **7**, e06379. https://doi.org/10.1016/j.heliyon.2021.e06379

[8] Huang, L., Sun, X., Li, C., Xu, R., Xu, J., Du, Y., *et al.* (2016) Electron Transport Layer-Free Planar Perovskite Solar Cells: Further Performance Enhancement Perspective from Device Simulation. *Solar Energy Materials and Solar Cells*, **157**, 1038-1047. https://doi.org/10.1016/j.solmat.2016.08.025

[9] Zhou, Q., Jiao, D., Fu, K., Wu, X., Chen, Y., Lu, J., *et al.* (2016) Two-Dimensional Device Modeling of $CH_3NH_3PbI_3$ Based Planar Heterojunction Perovskite Solar Cells. *Solar Energy*, **123**, 51-56. https://doi.org/10.1016/j.solener.2015.11.009

[10] Burgelman, M., Nollet, P. and Degrave, S. (2000) Modelling Polycrystalline Semiconductor Solar Cells. *Thin Solid Films*, **361**, 527-532. https://doi.org/10.1016/s0040-6090(99)00825-1

[11] Minemoto, T. and Murata, M. (2014) Device Modeling of Perovskite Solar Cells Based on Structural Similarity with Thin Film Inorganic Semiconductor Solar Cells. *Journal of Applied Physics*, **116**, Article ID: 054505. https://doi.org/10.1063/1.4891982

[12] Minemoto, T. and Murata, M. (2015) Theoretical Analysis on Effect of Band Offsets in Perovskite Solar Cells. *Solar Energy Materials and Solar Cells*, **133**, 8-14. https://doi.org/10.1016/j.solmat.2014.10.036

[13] Minemoto, T. and Murata, M. (2014) Impact of Work Function of Back Contact of Perovskite Solar Cells without Hole Transport Material Analyzed by Device Simulation. *Current Applied Physics*, **14**, 1428-1433. https://doi.org/10.1016/j.cap.2014.08.002

[14] Isoe, W., Mageto, M., Maghanga, C., Mwamburi, M., Odari, V. and Awino, C. (2020) Thickness Dependence of Window Layer on $CH_3NH_3PbI_{3-x}Cl_x$ Perovskite Solar Cell. *International Journal of Photoenergy*, **2020**, Article ID: 8877744. https://doi.org/10.1155/2020/8877744

[15] Green, M.A., Ho-Baillie, A. and Snaith, H.J. (2014) The Emergence of Perovskite Solar Cells. *Nature Photonics*, **8**, 506-514. https://doi.org/10.1038/nphoton.2014.134

[16] Grätzel, M. (2014) The Light and Shade of Perovskite Solar Cells. *Nature Materials*, **13**, 838-842. https://doi.org/10.1038/nmat4065

[17] Lee, M.M., Teuscher, J., Miyasaka, T., Murakami, T.N. and Snaith, H.J. (2012) Efficient Hybrid Solar Cells Based on Meso-Superstructured Organometal Halide Perovskites. *Science*, **338**, 643-647. https://doi.org/10.1126/science.1228604

[18] Stranks, S.D., Eperon, G.E., Grancini, G., Menelaou, C., Alcocer, M.J.P., Leijtens, T., *et al.* (2013) Electron-Hole Diffusion Lengths Exceeding 1 Micrometer in an Organometal Trihalide Perovskite Absorber. *Science*, **342**, 341-344. https://doi.org/10.1126/science.1243982

[19] Burschka, J., Pellet, N., Moon, S.J., Humphry-Baker, R., Gao, P., Nazeeruddin, M.K., *et al.* (2013) Sequential Deposition as a Route to High-Performance Perovskite-Sensitized Solar Cells. *Nature*, **499**, 316-319. https://doi.org/10.1038/nature12340

[20] Zhou, H., Chen, Q., Li, G., Luo, S., Song, T., Duan, H., *et al.* (2014) Interface Engineering of Highly Efficient Perovskite Solar Cells. *Science*, **345**, 542-546. https://doi.org/10.1126/science.1254050

[21] Tvingstedt, K., Malinkiewicz, O., Baumann, A., Deibel, C., Snaith, H.J., Dyakonov, V., *et al.* (2014) Radiative Efficiency of Lead Iodide Based Perovskite Solar Cells. *Scientific Reports*, **4**, Article No. 6071. https://doi.org/10.1038/srep06071

[22] Filipič, M., Löper, P., Niesen, B., De Wolf, S., Krč, J., Ballif, C., *et al.* (2015) $CH_3NH_3PbI_3$ Perovskite/Silicon Tandem Solar Cells: Characterization Based Optical Simulations. *Optics Express*, **23**, A263-A278. https://doi.org/10.1364/oe.23.00a263

[23] Sahu, A. and Dixit, A. (2018) Inverted Structure Perovskite Solar Cells: A Theoretical Study. *Current Applied Physics*, **18**, 1583-1591. https://doi.org/10.1016/j.cap.2018.10.008

[24] Lin, L., Jiang, L., Qiu, Y. and Yu, Y. (2017) Modeling and Analysis of HTM-Free Perovskite Solar Cells Based on ZnO Electron Transport Layer. *Superlattices and Microstructures*, **104**, 167-177. https://doi.org/10.1016/j.spmi.2017.02.028

[25] Ouédraogo, S., Traoré, B., Kébré, M.B., *et al.* (2020) Performance Enhancement Strategy of Ultra-Thin CIGS Solar Cells. *American Journal of Applied Sciences*, **17**, 246-

255. https://doi.org/10.3844/ajassp.2020.246.255

[26] Wanda, M.D., Ouédraogo, S., Tchoffo, F., Zougmoré, F. and Ndjaka, J.M.B. (2016) Numerical Investigations and Analysis of Cu_2ZnSnS_4 Based Solar Cells by SCAPS-1D. *International Journal of Photoenergy*, **2016**, Article ID: 2152018. https://doi.org/10.1155/2016/2152018

[27] Oubda, D., Kebre, M.B., Zougmore, F., Njomo, D. and Ouattara, F. (2015) Numerical Simulation of Cu(In, Ga)Se_2 Solar Cells Performances. *Journal of Energy and Power Engineering*, **9**, 1047-1055. https://doi.org/10.17265/1934-8975/2015.12.002